Induced Twisting in the Self-Assembly of Chiral Schiff-based Rod−Coil Amphiphiles

Chien-Hung Sung,[†] Liang-Rern Kung,[†] Chain-Shu Hsu,*,[†] Tz-Feng Lin,[‡] and Rong-Ming Ho*,[‡]

Department of Applied Chemistry, National Chiao Tung University, Hsinchu 30010, Taiwan, R.O.C., and Department of Chemical Engineering, National Tsing Hua University, Hsinchu 30013, Taiwan, R.O.C.

A series of novel organic superstructures exhibiting diverse aggregate morphologies with liquid-crystalline-like properties were prepared by a simple precipitation method. Here, a chiral sugar moiety was simply introduced at the Schiff-based rod end of rod−coil molecules. In contrast to coil−coil molecules, the self-assembled rod−coil molecules exhibit a high segregation strength for phase separation because of their liquid-crystalline-like behavior. The morphological transformation of self-assembled chiral Schiff-based rod−coil amphiphiles, from a platelet-like morphology to helical twists, was obtained by increasing the length of the hydrophobic tail. Consistent with theoretical predictions, the bending force from the chiral entity depends on the size of the adjacent hydrophobic tail. That is, the size of hydrophobic chain determines the threshold of bending for the formation of a helical morphology. Moreover, by introducing an additional tethered hydrophobic chain self-assembled spherical vesicles can be obtained through the collapse of the twisted shape.

Introduction

Nature elegantly utilizes the self-assembly of supramolecules to construct functional superstructures.[1−3] The self-assembled superstructures are formed by cooperative secondary forces such as amphiphilic effects, polarizability, hydrogen bonding, Coulombic interactions, van der Waals forces, metal coordination, ionic bonding, and chirality. On the basis of many systematic experiments, Kunitake and co-workers reported the relationship between the structures of synthetic bilayer-forming compounds and the resulting self-assembled morphologies.[4−6] The self-assembly behaviors of the synthetic compounds depend on molecular functionalities necessary for aggregation and the location and orientation of these functionalities.[7,8] Among the factors supporting self-assembly, the chiral effects have been demonstrated to be one of the important driving forces for the formation of helical morphologies.[9−15] A variety of helical morphologies including helical conformations, hierarchical helical struc-

tures, and helical crystalline morphologies have been observed.[16−23] Nelson and co-workers presented the design and characterization of helix-forming oligomers whose ordered conformations are stabilized by "nonspecific" forces.[21] Subsequently, a successful foldamer (any oligomer that folds into a conformationally ordered state in solution stabilized by a collection of noncovalent interactions between nonadjacent monomer units) was obtained by Moore and co-workers.[22] Recently, helical superstructures with nanoscale dimensions have been obtained from the self-assembly of block copolymers containing chiral blocks (i.e., chiral coil−coil supramolecules) in buffer solutions[24] and in the bulk.[25] The chiral effect on the self-assembly of block copolymers

---

* To whom correspondence should be addressed. Tel.: 886-3-5712121-31523 (C.-S.H.), 886-3-5738349 (R.-M.H.). Fax: 886-3-5723764 (C.-S.H.), 886-3-5715408 (R.-M.H.). E-mail: cshsu@mail.nctu.edu.tw (C.-S.H.), rmho@mx.nthu.edu.tw (R.-M.H.).

† National Chiao Tung University.
‡ National Tsing Hua University.

(1) Whitesides, G. M.; Grzybowski, B. *Science* **2002**, *295*, 2418.
(2) Aggeli, A.; Nyrkova, I. A.; Bell, M.; Harding, R.; Carrick, L.; Mcleish, T. C. B.; Semenov, A. N.; Boden, N. *Proc. Natl. Acad. Sci. U.S.A.* **2001**, *98*, 11857.
(3) Lehn, J. M. *Supramolecular Chemistry*; VCH: Weinheim, Germany, 1995.
(4) Kunitake, T.; Okahata, Y. *J. Am. Chem. Soc.* **1980**, *102*, 549.
(5) Kunitake, T.; Okahata, Y.; Shimomura, M.; Yasunami, S.; Takarabe, K. *J. Am. Chem. Soc.* **1981**, *103*, 5401.
(6) Kunitake, T. *Angew. Chem., Int. Ed. Engl.* **1992**, *31*, 709.
(7) Whitesides, G. M.; Mathias, J. P. *Science* **1991**, *254*, 1312.
(8) Chandross, E. A.; Miller, R. D. *Chem. Rev.* **1999**, *99*, 1641.
(9) Zhang, J.; Wang, Z. L.; Liu, J.; Chen, S.; Liu, G. Y. *Self-Assembled Nanostructures*; Kluwer Academic: New York, 2003.
(10) Estroff, L. A.; Hamilton, A. D. *Chem. Rev.* **2004**, *104*, 1201.

(11) Li, C. Y.; Cheng, S. Z. D. Ge, J. J.; Bai, F.; Zhang, J. Z.; Mann, I. K.; Harris, F. W.; Chien, L. C.; Yan, D.; He; Lotz, B. *Phys. Rev. Lett.* **1999**, *83*, 4558.
(12) Tachibana, T.; Kambara, H. *J. Am. Chem. Soc.* **1965**, *87*, 3015.
(13) Vriezema, D. M.; Hoogboom, J.; Velonia, K.; Takazawa, K.; Christianen, P. C. M.; Maan, J. C.; Rowan, A. E.; Nolte, R. J. M. *Angew. Chem., Int. Ed.* **2003**, *42*, 772.
(14) Li, B. S.; Cheuk, K. L.; Salhi, F.; Lam, J. W. Y.; Cha, J. A. K.; Xiao, X.; Bai, C.; Tang, B. Z. *Nano Lett.* **2001**, *1*, 323.
(15) Goodby, J. W.; Waugh, M. A.; Stein, S. M.; Chin, E.; Pindak, R.; Patel, J. S. *J. Am. Chem. Soc.* **1989**, *111*, 8119.
(16) Nakashima, N.; Asakuma, S.; Kunitake, T. *J. Am. Chem. Soc.* **1985**, *107*, 509.
(17) Fuhrhop, J. H.; Helfrich, W. *Chem. Rev.* **1993**, *93*, 1565.
(18) Boettcher, C.; Schade, B.; Fuhrhop, J. H. *Langmuir* **2001**, *17*, 873.
(19) Brunsveld, L.; Vekemans, J. A. J. M.; Hirschberg, J. H. K. K.; Sijbesma, R. P.; Meijer, E. W. *Proc. Natl. Acad. Sci. U.S.A.* **2001**, *99*, 4977.
(20) Petitjean, A.; Nierengarten, H.; Dorsselaer, A. V.; Lehn, J. M. *Angew. Chem., Int. Ed.* **2004**, *43*, 3695.
(21) Nelson, J. C.; Saven, J. G.; Moore, J. S.; Wolynes, P. G. *Science* **1997**, *277*, 1793.
(22) Hill, D. J.; Mio, M. J.; Prince, R. B.; Hughes, T. S.; Moore, J. S. *Chem. Rev.* **2001**, *101*, 3893.
(23) Cornelissen, J. J. L. M.; Fischer, M.; Sommerdijk, N. A. J. M.; Nolte, R. J. M. *Science* **1998**, *280*, 1427.
(24) . Rowan, A. E.; Nolte, R. J. M. *Angew. Chem,. Int. Ed.* **1998**, *37*, 63.
(25) Ho, R. M.; Chiang, Y. W.; Tsai, C. C.; Lin, C. C.; Ko, B. T.; Huang, B. H. *J. Am. Chem. Soc.* **2004**, *126*, 2704.

Self-Assembly of Chiral Schiff-based Rod−Coil Amphiphiles

Chem. Mater., Vol. 18, No. 2, 2006 353

is essential for the formation of a helical morphology. In contrast to coil−coil molecules, the self-assembly of rod−coil molecules also exhibits periodic textures even for oligomeric molecules because of the large persistent length of the rod segment.

Amphiphilic molecules offer numerous opportunities for chemical variations and thus provide a crucial direction for the controlled fabrication of superstructures. The self-assembly of lipid bilayers (i.e., amphiphiles) has been extensively studied, and a variety of dynamically changing morphologies in the liquid-crystalline (fluid) state have been observed.[26−28] For example, Fuhrhop and co-workers demonstrated that the solubilities and aggregate structures of aldonamide depend directly on the stereochemistry of the polyol headgroups. Undisturbed all-anti chains lead to bimolecular sheets, whereas a bend close to the amide group produces cylindrical micelles with high curvature, and a twist at the end of the chain causes the amphiphiles to be water-soluble and prevents fiber formation.

Among the chiral amphiphiles whose self-assembly has been studied, carbohydrate sugars provide a rich library of chiral building blocks that are also biocompatible, which makes them attractive candidates for use in the design of self-assembly chemistry for bioapplications.[29] Shinkai and co-workers have made the most extensive use of sugars in their quest for small-molecule organic hydrogelators. The morphologies of sugar-based amphiphiles, affected by the introduction of different hydrophilic or hydrophobic parts[30−34] and by unsaturation in the lipophilic moiety, have been thoughtfully studied by Shimizu and co-workers.[35,36] The self-assembly of unsaturated alkyl chains of glycolipids exhibited an interesting self-assembled conversion from coiled nanofibers gradually to a tubular morphology.

In this study, a sugar entity (i.e., a chiral entity) was introduced at the rod end of rod−coil molecules having a Schiff-based rod and a hydrophobic alkoxyl tail. The amphiphilic Schiff-based molecules having an alkoxyl chain and a glucoside moiety on the opposite sides were obtained in a multiple synthesis. A series of chiral Schiff-based rod−coil amphiphiles with different alkoxyl chain lengths were thus prepared (Figure 1). The self-assembly of chiral rod−coil molecules having amphiphilic characters gave rise to the formation of interesting aggregates in aqueous solution. The morphological transformation from a platelet-like mor-
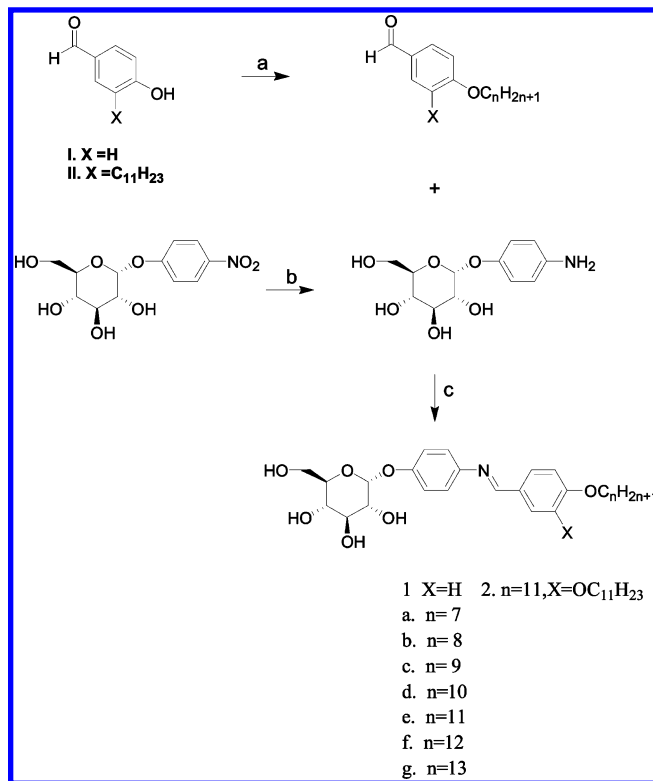

Figure 1. Synthetic routes and chemical structures of chiral rod−coil molecules.

phology to helical twists was obtained by simply increasing the length of the hydrophobic chain in the chiral Schiff-based rod−coil amphiphiles, suggesting a general rule for the formation of a helical morphology from chiral amphiphiles. The formation of helical twists is attributed to the introduction of bending and twisting forces through the sugar-based chiral entity. Moreover, self-assembled spherical vesicles can also be obtained by introducing an additional tethered long alkoxyl chain.

Experimental Section

Materials. The synthetic routes and chemical structures of chiral Schiff-based amphiphiles are shown in Figure 1. The resulting amphiphilic Schiff-based species **1** and **2** were characterized by ¹H and ¹³C NMR spectroscopy, elemental analysis, and high-resolution mass spectroscopy and shown to be in full agreement with the structures presented.

The mono- and dialkoxylbenzaldehyde compounds were prepared using a typical esterification method. An example for the synthesis of 4-undecyloxylbenzaldehyde ($n = 11$) is described as follows: 4-Hydroxybenzaldehyde (3.0 g, 24.6 mmol), K_2CO_3 (8.4 g, 61.5 mmol), and KI (0.05 g, 0.3 mmol) were mixed into 30 mL of acetone. The solution was heated to reflux temperature and then stirred for 30 min under nitrogen gas. 1-Bromoundecane (6.36 g, 27.1 mmol) was slowly added, and then the reaction mixture was refluxed for an additional 12 h. After being allowed to cool, the solution was filtered to remove solid salt and then evaporated under reduced pressure to give the crude oil product. Further purification was performed using liquid chromatography (silica gel, with a 1:5 mixture of EtOAc/*n*-hexane as the eluent) to give an oil product (6.1 g, 90%).

4-Undecanoxybenzaldehyde. ¹H NMR (CDCl₃) δ (ppm): 9.83 (s, 1H), 7.77 (d, 2H, $J = 6.3$ Hz), 6.95 (d, 2H, $J = 8.4$ Hz), 3.99 (t, 2H, 6.6 Hz), 1.77 (m, 2H), 1.41 (m, 16H), 0.85 (t, 3H, 6.6 Hz).

(26) Fuhrhop, J. H.; Schnieder, P.; Boekema, E.; Helfrich, W. *J. Am. Chem. Soc.* **1988**, *110*, 2861.
(27) Spector, M. S.; Selinger, J. V.; Singh, A.; Rodriguez, J. M.; Price, R. R.; Schnur, J. M. *Langmuir* **1998**, *14*, 3493.
(28) Spector, M. S.; Price, R. R.; Schnur, J. M. *Adv. Mater.* **1999**, *11*, 337.
(29) Gronwald, O.; Shinkai, S. *Chem. Eur. J.* **2001**, *7*, 4328.
(30) Van Doren, H. A.; Smits, E.; Pestman, J. M.; Engberts, J. B. F. N.; Kellogg, R. M. *Chem. Soc. Rev.* **2000**, *29*, 183.
(31) Laurent, N.; Lafon, D.; Dumoulin, F.; Boullanger, P.; Mackenzie, G.; Kouwer, P. H. J.; Goodby, J. W. *J. Am. Chem. Soc.* **2003**, *125*, 15499.
(32) Jenekhe, S. A.; Chen, X. L. *Science* **1998**, *279*, 1903.
(33) Jung, J. H.; Yoshida, K.; Shimizu, T. *Langmuir* **2002**, *18*, 8724.
(34) Shimizu, T.; Masuda, M.; Minamikawa, H. *Chem. Rev.* **2005**, *105*, 1401.
(35) John, G.; Masuda, M.; Okada, Y.; Yase, K.; Shimizu, T. *Adv. Mater.* **2001**, *13*, 715.
(36) John, G.; Jung, J. H.; Minamikawa, H.; Yoshida, K.; Shimizu, T. *Chem. Eur. J.* **2002**, *8*, 5495.

^{13}C NMR (CDCl$_3$) δ (ppm): 190.80, 163.18, 132.95, 130.92, 114.90, 68.45, 31.79, 29.72, 29.55, 28.90, 28.72, 26.57, 25.87, 22.65, 14.16.

3,4-Diundecanoxybenzaldehyde. ^{1}H NMR (CDCl$_3$) δ (ppm): 9.92 (s, 1H), 7.42 (d, 1H, J = 7.5 Hz), 7.39 (s, 1H), 6.95 (d, 1H, J = 7.8 Hz), 4.07 (m, 4H), 1.85 (m, 4H), 1.42 (m, 32H), 0.87 (t, 6H, 6.9 Hz). ^{13}C NMR (CDCl$_3$) δ (ppm): 190.82, 163.18, 132.95, 130.91, 123.82, 112.57, 111.42, 68.43, 31.79, 29.72, 29.55, 28.90, 28.72, 26.57, 25.87, 22.65, 14.16.

(4-Aminophenyl)-α-D-glucopyranoside. A calatytic amount of Pd/C (10%) (ca. 1 mg) was added to a solution of (4-nitrophenyl)-α-D-glucopyranoside (0.5 g, 1.66 mmol) in mL THF/water (9:1) at ambient temperature under hydrogen atmosphere. After 3 h of stirring under H$_2$(g), the mixture was filtered and concentrated in vacuo to yield the amine (0.4 g, 88%) as a white solid. ^{1}H NMR (DMSO-d_6) δ (ppm): 6.76 (d, 2H, J = 6.3), 6.44 (d, 2H, J = 4.5 Hz), 5.04 (m, 1H), 4.90 (m, 2H), 4.82 (d, 1H, J = 4.8 Hz), 4.67 (s, 2H), 4.44 (m, 1H), 3.57 (m, 4H), 3.23 (m, 1H), 3.10 (m, 1H). ^{13}C NMR (DMSO-d_6) δ (ppm): 149.06, 144.48, 119.45, 115.22, 100.23, 74.00, 73.85, 72.49, 70.82, 61.47.

A typical procedure for the preparation of Schiff-based molecules is described below. DMSO (0.5 mL) was added to 10 mL of a THF solution containing 1 mmol of (4-aminophenyl)-α-d-glucopyranoside and 1 mmol of 4-alkoxybenzaldehyde under nitrogen atmosphere. The resulting mixture was heated in an oil bath (100 °C) and continuously stirred until the amine and aldehyde had been consumed, as confirmed by TLC analysis. After being allowed to cool, the mixture was washed with water, and followed the solvent was extracted. The resulting residue was recrystallized in hot ethyl acetate to obtain the imine **1**.

4-Heptyloxybenzylidene Aminophenyl-α-D-glucopyranoside (1a). ^{1}H NMR (DMSO-d_6) δ (ppm): 8.51 (s, 1H), 7.82 (d, 2H, J = 8.7 Hz), 7.22 (d, 2H, J = 9 Hz), 7.11 (d, 2H, J = 8.7 Hz), 7.03 (d, 2H, J = 8.7 Hz), 5.36 (d, 1H, J = 3.3 Hz), 5.09 (d, 1H, J = 6.3 Hz), 4.99 (d, 1H, J = 5.7 Hz), 4.95 (d, 1H, J = 5.1 Hz), 4.50 (t, 1H, J = 5.1 Hz), 3.99 (t, 2H, J = 6.6 Hz), 3.58−3.54 (m, 2H), 3.47 (d, 1H, J = 8.4 Hz), 3.18 (m, 1H), 1.70 (q, 2H, J = 6.9 Hz), 1.37 (m, 8H), 0.84 (t, 3H, J = 6.9 Hz). ^{13}C NMR (DMSO-d_6) δ (ppm): 160.66, 157.83, 154.96, 145.28, 129.74, 128.49, 121.54, 117.14, 114.16, 97.80, 73.24, 72.59, 71.15, 69.45, 67.20, 60.22, 30.82, 28.51, 28.31, 28.20, 28.13, 25.01, 21.64, 13.50. ESI mass: 473.24. Anal. Calcd (%) for C$_{26}$H$_{35}$NO$_7$ (473.24): C, 65.94; H, 7.45; N, 2.96. Found: C, 64.51; H, 7.91; N, 2.99.

4-Octyloxybenzylidene Aminophenyl-α-D-glucopyranoside (1b). ^{1}H NMR (DMSO-d_6) δ (ppm): 8.51 (s, 1H), 7.83 (d, 2H, J = 9 Hz), 7.22 (d, 2H, J = 9 Hz), 7.11 (d, 2H, J = 8.7 Hz), 7.03 (d, 2H, J = 8.7 Hz), 5.35 (d, 1H, J = 3.9 Hz), 5.06 (d, 1H, J = 6.3 Hz), 4.98 (d, 1H, J = 5.7 Hz), 4.96 (d, 1H, J = 5.1 Hz), 4.48 (t, 1H, J = 5.1 Hz), 3.99 (t, 2H, J = 6.6 Hz), 3.58−3.54 (m, 2H), 3.47 (d, 1H, J = 8.4 Hz), 3.18 (m, 1H), 1.71 (m, 2H), 1.27 (m, 10H), 0.84 (t, 3H, J = 6.9 Hz). ^{13}C NMR (DMSO-d_6) δ (ppm): 161.83, 158.99, 156.12, 146.45, 130.90, 129.66, 122.69, 118.32, 115.34, 98.99, 74.41, 73.76, 72.32, 70.65, 68.37, 61.39, 31.92, 29.42, 29.35, 29.28, 26.18, 22.78, 14.66.

4-Nonyloxybenzylidene Aminophenyl-α-D-glucopyranoside (1c). ^{1}H NMR (DMSO-d_6) δ (ppm): 8.51 (s, 1H), 7.82 (d, 2H, J = 9 Hz), 7.22 (d, 2H, J = 9 Hz), 7.08 (d, 2H, J = 6.6 Hz), 7.01 (d, 2H, J = 8.7 Hz), 5.35 (d, 1H, J = 3.6 Hz), 5.07 (d, 1H, J = 6.3 Hz), 4.99 (d, 1H, J = 5.7 Hz), 4.95 (d, 1H, J = 4.8 Hz), 4.49 (t, 1H, J = 5.1 Hz), 4.01 (t, 2H, J = 6.3 Hz), 3.58−3.53 (m, 2H), 3.47 (d, 1H, J = 8.4 Hz), 3.19 (m, 1H), 1.70 (q, 2H, J = 7.2 Hz), 1.37 (m, 12H), 0.83 (t, 3H, J = 6.9 Hz). ^{13}C NMR (DMSO-d_6) δ (ppm): 160.66, 157.82, 154.96, 145.28, 129.74, 128.49, 121.54, 117.15, 114.15, 97.81, 73.24, 72.60, 71.15, 69.46, 67.20, 60.22,

30.78, 28.14, 27.99, 24.99, 21.61, 13.50. ESI mass: 501.27. Anal. Calcd (%) for C$_{28}$H$_{39}$NO$_7$ (501.27): C, 67.04; H, 7.84; N, 2.79. Found: C, 67.07; H, 7.69; N, 2.9.

4-Decyloxybenzylidene Aminopheny-α-D-glucopyranoside (1d). ^{1}H NMR (DMSO-d_6) δ (ppm): 8.51 (s, 1H), 7.83 (d, 2H, J = 8.7 Hz), 7.22 (d, 2H, J = 9 Hz), 7.11 (d, 2H, J = 8.7 Hz), 7.03 (d, 2H, J = 8.7 Hz), 5.35 (d, 1H, J = 3.9 Hz), 5.06 (d, 1H, J = 6.3 Hz), 4.98 (d, 1H, J = 5.7 Hz), 4.96 (d, 1H, J = 5.1 Hz), 4.49 (t, 1H, J = 5.4 Hz), 4.01 (t, 2H, J = 6.6 Hz), 3.60−3.54 (m, 2H), 3.48 (d, 1H, J = 8.4 Hz), 3.18 (m, 1H), 1.71 (m, 2H), 1.27 (m, 14H), 0.84 (t, 3H, J = 6.9 Hz). ^{13}C NMR (DMSO-d_6) δ (ppm): 161.82, 158.98, 156.12, 146.45, 130.89, 129.66, 122.69, 118.31, 115.34, 98.99, 74.41, 73.76, 72.32, 70.64, 68.37, 61.39, 31.99, 29.69, 29.65, 29.45, 29.40, 29.27, 26.16, 22.79, 14.66.

4-Undecyloxybenzylidene Aminophenyl-α-D-glucopyranoside (1e). ^{1}H NMR (DMSO-d_6) δ (ppm): 8.49 (s, 1H), 7.82 (d, 2H, J = 9 Hz), 7.20 (d, 2H, J = 9 Hz), 7.10 (d, 2H, J = 6.9 Hz), 7.02 (d, 2H, J = 8.1 Hz), 5.33 (d, 1H, J = 3.6 Hz), 5.05 (d, 1H, J = 6.3 Hz), 4.97 (d, 1H, J = 5.7 Hz), 4.92 (d, 1H, J = 4.8 Hz), 4.48 (t, 1H, J = 5.1 Hz), 4.00 (t, 2H, J = 6.0 Hz), 3.59−3.53 (m, 2H), 3.45 (d, 1H, J = 8.4 Hz), 3.18 (m, 1H), 1.69 (q, 2H, J = 7.2 Hz), 1.38 (m, 16H), 0.82 (t, 3H, J = 6.3 Hz). ^{13}C NMR (DMSO-d_6) δ (ppm): 160.66, 157.82, 154.96, 145.28, 129.74, 128.48, 121.54, 117.15, 114.16, 97.81, 73.24, 72.60, 71.15, 69.46, 67.20, 60.22, 30.78, 28.14, 27.99, 24.99, 21.61, 13.50. ESI mass: 529.30. Anal. Calcd (%) for C$_{30}$H$_{43}$NO$_7$ (529.30): C, 68.03; H, 8.18; N, 2.64. Found: C, 67.85; H, 8.11; N, 2.75.

4-Dodecyloxybenzylidene Aminophenyl-α-D-glucopyranoside (1f). ^{1}H NMR (DMSO-d_6) δ (ppm): 8.51 (s, 1H), 7.84 (d, 2H, J = 8.4 Hz), 7.22 (d, 2H, J = 5.4 Hz), 7.11 (d, 2H, J = 8.7 Hz), 7.03 (d, 2H, J = 8.7 Hz), 5.36 (d, 1H, J = 3.9 Hz), 5.06 (d, 1H, J = 6.3 Hz), 4.98 (d, 1H, J = 5.4 Hz), 4.96 (d, 1H, J = 7.8 Hz), 4.50 (t, 1H, J = 5.4 Hz), 3.99 (t, 2H, J = 6.6 Hz), 3.62−3.57 (m, 2H), 3.48 (d, 1H, J = 8.4 Hz), 3.21 (m, 1H), 1.70 (m, 2H), 1.22 (m, 18H), 0.84 (t, 3H, J = 6.9 Hz). ^{13}C NMR (DMSO-d_6) δ (ppm): 161.82, 158.96, 156.13, 146.45, 130.89, 129.66, 122.67, 118.31, 115.32, 98.98, 74.40, 73.76, 72.32, 70.63, 68.35, 61.38, 31.99, 29.70, 29.67, 29.41, 29.26, 29.14, 22.79, 14.65.

4-Tridecyloxybenzylidene Aminophenyl-α-D-glucopyranoside (1g). ^{1}H NMR (DMSO-d_6) δ (ppm): 8.51 (s, 1H), 7.84 (d, 2H, J = 8.7 Hz), 7.22 (d, 2H, J = 6.6 Hz), 7.11 (d, 2H, J = 6.6 Hz), 7.03 (d, 2H, J = 9 Hz), 5.36 (d, 1H, J = 3.9 Hz), 5.06 (d, 1H, J = 6.0 Hz), 4.98 (d, 1H, J = 5.7 Hz), 4.96 (d, 1H, J = 7.8 Hz), 4.48 (t, 1H, J = 5.4 Hz), 4.00 (t, 2H, J = 6.6 Hz), 3.62−3.54 (m, 2H), 3.48 (d, 1H, J = 8.4 Hz), 3.20 (m, 1H), 1.73 (m, 2H), 1.22 (m, 20H), 0.84 (t, 3H, J = 6.9 Hz). ^{13}C NMR (DMSO-d_6) δ (ppm): 161.82, 158.96, 156.13, 146.45, 130.89, 129.66, 122.68, 118.31, 115.32, 98.99, 74.40, 73.76, 72.32, 70.64, 68.35, 61.38, 31.99, 29.75, 29.71, 29.67, 29.41, 29.27, 26.15, 22.79, 19.38, 14.65.

3,4-Diundecyloxybenzylidene Aminophenyl-α-D-glucopyranoside (2). DMSO (0.5 mL) was added to 10 mL of a THF solution containing 1 mmol of (4-aminophenyl)-α-d-glucopyranoside and 1 mmol of 3,4-diundecyloxybenzaldehyde under nitrogen atmosphere. The resulting mixture was heated in an oil bath (100 °C) and continuously stirred until the amine and aldehyde had been consumed, as confirmed by TLC analysis. After being allowed to cool, the mixture was washed with water, and the solvent was extracted. The resulting residue was recrystallized in hot ethyl acetate to obtain the imine **2**.

^{1}H NMR (DMSO-d_6) δ (ppm): 8.45 (s, 1 H), 7.48 (s, 1H), 7.37 (d, 1H, J = 8.1 Hz), 7.20 (d, 2H, J = 9 Hz), 7.10 (d, 2H, J = 6.6 Hz), 6.99 (d, 1H, J = 8.4 Hz), 5.35 (d, 1H, J = 3.6 Hz), 5.06 (d, 1H, J = 6.3 Hz), 4.99 (d, 1H, J = 5.7 Hz), 4.94 (d, 1H, J = 5.1 Hz), 4.48 (t, 1H, J = 5.7 Hz), 3.95 (t, 4H, J = 6.0 Hz), 3.59−3.53

Self-Assembly of Chiral Schiff-based Rod−Coil Amphiphiles

Chem. Mater., Vol. 18, No. 2, 2006 355

(m, 2H), 3.45 (d, 1H, J = 8.4 Hz), 1.66 (m, 4H), 1.40 (m, 4H), 1.20 (m, 28H), 0.81 (t, 6H, J = 6.3 Hz). ^{13}C NMR (DMSO-d_6) δ (ppm): 158.45, 156.22, 151.46, 145.72, 129.25, 123.65, 121.75, 117.65, 112.65, 111.31, 98.33, 73.70, 73.07, 71.64, 69.92, 68.31, 60.69, 40.33, 40.06, 39.78, 39.50, 39.22, 38.94, 38.66, 35.15, 30.44, 29.18, 29.15, 29.11, 28.91, 28.83, 28.75, 27.22, 25.65, 22.14, 21.81, 6.84. ESI mass: 699.47. Anal. Calcd (%) for $C_{41}H_{65}NO_8$ (699.47): C, 70.35; H, 9.36; N. 2.0. Found: C, 70.33; H, 9.32; N, 2.35.

Characterization Techniques. The chiral Schiff-based rod−coil amphiphiles were aggregated in dilute solution by using 1 mg of compound dissolved in 1 mL of tetrahydrofuran, and then introducing 9 mL of deionized water into the well-dissolved solution. After sufficient time for aggregation, a drop of the mixture was transferred to carbon film. The cast samples were then examined by field-emission scanning electron microscopy (FESEM) and transmission electron microscopy (TEM). Bright-field TEM images were obtained on a JEOL TEM-1200x transmission electron microscopy. The quenched samples were shadowed by Pt and coated with carbon again. After being shadowed, the specimens were stripped and floated onto the water surface and then recovered using copper grids. Field-emission scanning electron microscopy was performed on a JEOL JSM-6700F using accelerating voltages of 0.5−1 keV. The samples were mounted to brass shims using carbon adhesive and then sputter-coated with 2−3 nm of gold (the gold coating thickness was estimated from the calculated deposition rate and experimental deposition time).

Thermal transitions and properties of samples were determined using a Perkin-Elmer Pyris 1 differential scanning calorimeter equipped with a liquid nitrogen cooling accessory. A 3−6-mg sample of purified material was placed on an aluminum pan and measured against another empty pan as a reference. The thermograms were recorded at a heating/cooling rate of 20 °C/min. A Carl-Zeiss Axiphot optical polarized microscope equipped with a Mettler FP82 hot stage and a FP80 central processor were used to observe the thermal transitions and to analyze the anisotropic textures. UV−vis absorption spectra were recorded on a Hitachi U-3300 spectrophotometer. Circular dichroism (CD) measurements were conducted on a JASCO J-720 spectrophotometer. UV−vis and CD spectroscopy measurements were performed to investigate the specific interactions and the chiral expression of the samples in solution. The spectroscopic experiments were carried out in THF solution (concentration = 1 × 10^{-4} M). Infrared (IR) spectra were obtained using a Perkin-Elmer series FT-IR spectrophotometer at a resolution of 1.0 cm^{-1}. The scanned wavenumber range was 4000−400 cm^{-1}. Measurements were studied to discriminate the intermolecular hydrogen-bonding interactions in pure THF and THF/H$_2$O solution. For experiment a, 1 mg of compound **1e** was dissolved in 10 mL of purified THF, and then 3 drops of the solution were cast and dried on the transparent potassium bromide salt plate. In experiment b, 1 mg of compound **1e** was dissolved in 1 mL of THF and then mixed with 9 mL of distilled water to obtain a uniform solution (1:9 v/v). After a 24-h aggregation process, 3 drops of this solution were cast on potassium salt plate and then dried on a vacuum system for 12 h before measurement.

Molecular Simulation. Mechanisms of self-assembly were studied by considering the interaction of secondary forces through the aid of molecular simulation. The energy minimization of self-assembled morphology was implemented using HyperChem 7 through the OPLS force field to examine the possible mechanisms, especially the chiral effect on self-assembly. Because the OPLS force field is based on a biomolecular database, it should be suitable for use in studying the chiral effect on chiral Schiff-based rod−coil amphiphiles. The Monte Carlo method was used to search for stable structures from several different initial conformations.

Results and Discussion

Self-Assembly Process of Chiral Schiff-Based Amphiphiles in Solution. The self-assembled morphologies of sugar-based amphiphiles including twisted fibers, coiled tubes, and helical ribbons have been extensively studied recently.[37] The aggregate superstructures are, in general, driven by the liquid-crystalline-like behavior of the rod segments in the sugar-based amphiphiles, whereas the formation of a helical morphology is related to the chiral effect of sugar-based entity. To examine the origin of helix formation, in particular the bending and twisting forces of bilayered aggregates driven by a chiral entity (i.e., the effect of the chain length of the hydrophobic tail), a convenient synthetic method known as the "Schiff-based reaction" to combine a hydrophilic sugar base with a hydrophobic lipid moiety to form an imine linkage as a rigid spacer for self-assembly was utilized. As expected, all of the synthesized products having a variety of alkoxyl chain lengths exhibited thermotropic liquid-crystalline properties as identified by DSC thermograms and polarized light microscopy.[38]

One of the most convenient techniques for evolving hierarchical superstructures from a bottom-up approach is to carry out self-assembly in the solution state. Moreover, the self-assembly mechanism can thus be clearly elucidated by tracing the development of the morphology from the molecular level to the hierarchical ensemble. To examine the chiral character of the sugar-based entity, UV−vis and CD experiments of THF and aqueous solutions of chiral Schiff-based rod−coil amphiphiles were preformed first. For comparison, the starting material, 4-nitrophenyl-α-d-glucopyranoside (4-NADG), with 99% dextrorotatory conformation, was dissolved in solvent to form solutions (1 mg/10 mL) for spectroscopic measurements. As shown in Figure 2a, the maximum absorption of the $\pi-\pi$ transition appears in the UV−vis spectrum at 299 nm in THF solution, whereas a red shift of the maximum absorption to 304 nm can be identified as a result of the hydrogen bonding of the carbohydrate sugar with water in aqueous solution. Corresponding CD results (Figure 2b) indicate that the starting material, 4-NADG, displays a typical positive Cotton effect whether in THF or in water. That is, 4-NADG exhibits typical spectroscopic results as chiral character. UV−vis spectra of chiral Schiff-based rod−coil amphiphiles with various alkoxy chain lengths (n = 7−13) in THF were then obtained (as shown in Figure 3a). Two absorption bands at 280 and 330 nm appear as a result of $\pi-\pi^*$ and $n-\pi^*$ transitions related to π and nonbonding electron absorption, respectively. The band attributed to a $\pi-\pi^*$ transition at 280 nm provides evidence of $\pi-\pi$ interactions between the phenyl groups, whereas the band attributed to a $n-\pi^*$ transition at 330 nm suggests a contribution due to hydrogen bonding. As for the starting material 4-NADG, a positive Cotton effect was exhibited, as evidenced by CD absorptions, suggesting the preservation of the chiral expression of the sugar-based entity in the chiral Schiff-based rod−coil amphiphiles. Consistent results in both UV−vis and CD spectra can be obtained

(37) Jung, J. H.; John, G.; Yoshida, K.; Shimizu, T. *J. Am. Chem. Soc.* **2002**, *124*, 10674.
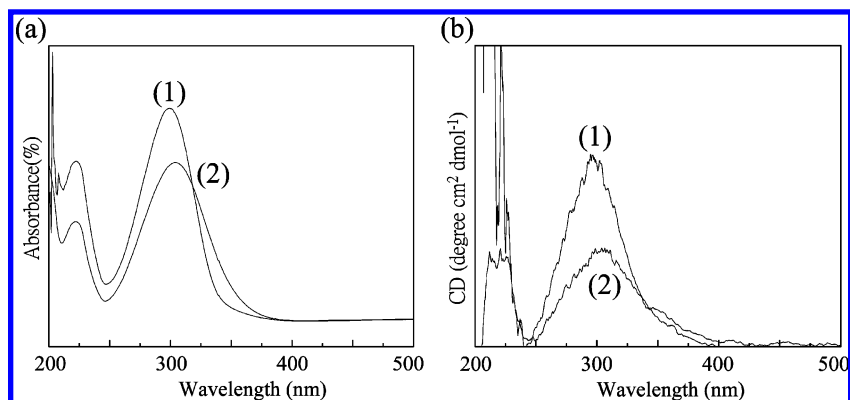(38) Sung, C. H.; Kung, L. R.; Hsu, C. S.; Lin, T. F.; Ho, R. M. *Liq. Cryst.*, manuscript in preparation.

Figure 2. Corresponding (a) UV−vis spectra and (b) CD results of 4-NADG in (1) THF and (2) water.
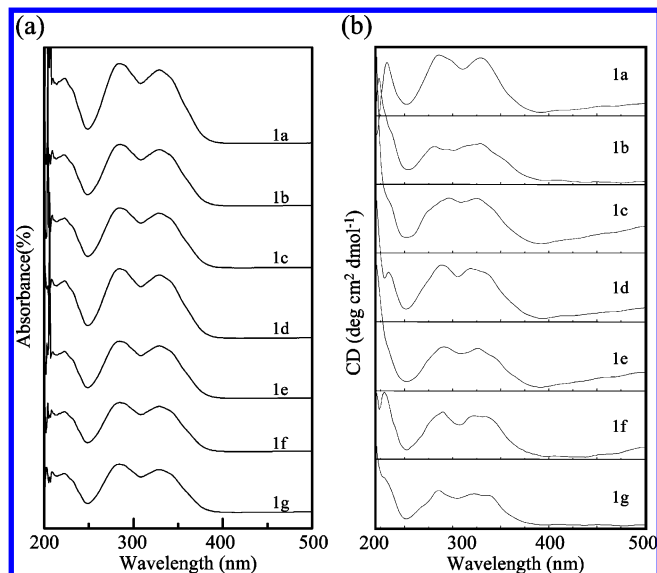

Figure 3. (a) UV−vis and (b) CD spectra of compounds **1a−1g** in THF.

Figure 4. Time-resolved UV−vis spectra of compound **1e** in THF/H_2O.
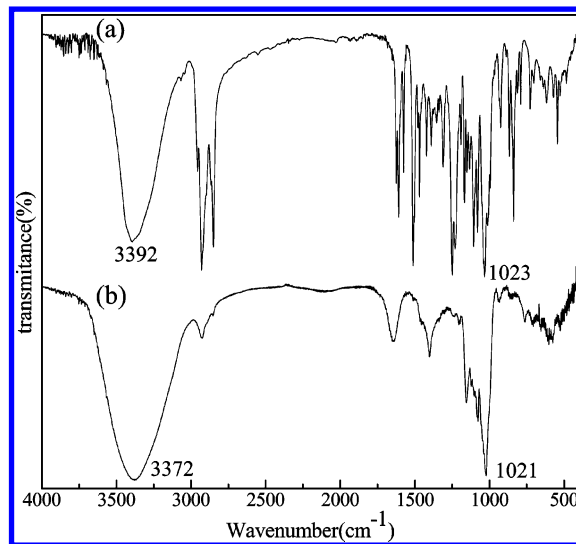
Figure 5. FT-IR spectra of compound **1e** in (a) pure THF and (b) THF/H_2O solution.

regardless of the change in chain length for the synthesized chiral amphiphiles, reflecting the likelihood that bending and twisting forces driven by the sugar-based chiral entity can be anticipated in the self-assembly process.

To monitor the evolution of the self-assembled morphology, time-resolved UV−vis experiments were carried out in the mixed solvent system (i.e., THF/H_2O) so that the self-assembly mechanism could be examined in the presence of H_2O. 4-Undecyloxybenzlidene aminophenyl-α-d-glucopyranoside (1 mg, compound 1e) was dissolved in 1 mL of THF mixed with 9 mL H_2O (1:9 v/v), and then the solution was immediately used for time-resolved UV−vis experiments. As illustrated in Figure 4 for compound 1e, the 280-nm $\pi-\pi^*$ transition remains throughout the self-assembly process with time evolution, but a blue shift gradually occurs for the $n-\pi^*$ transition from 330 to 290 nm, suggesting a hypsochromic shift[39,40] resulting from dipole−dipole interactions and hydrogen-bond formation. Consistently, the imine group appears as a $\pi-\pi^*$ transition in the near-UV region at about 230 nm that shows an obvious intensification at the end of aggregation because of the hydrogen-bonding enhancement. As a result, we speculate that the aggregation is indeed initiated by the Schiff-based rod entity (i.e., the liquid-
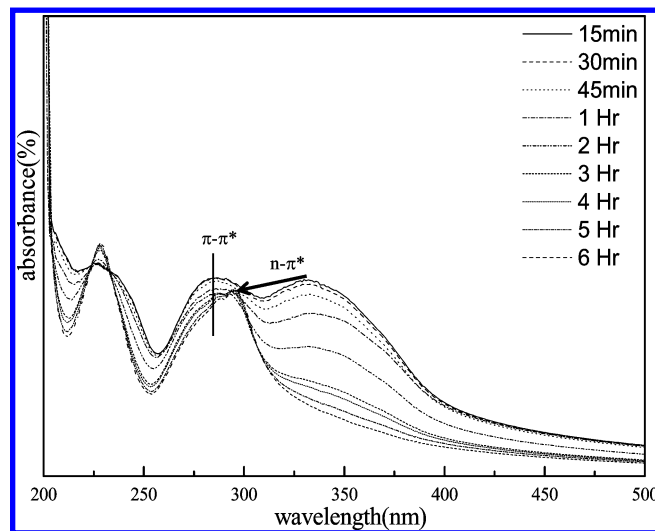
crystalline-like behavior) as a result of the induction of the hydrogen-bonding interaction and that the introduction of water might promote the self-assembly process. To further confirm the intermolecular hydrogen-bonding interaction and the participation of water in the self-assembly process, FTIR experiments were conducted. As illustrated in Figure 5a, the spectrum of compound 1e shows a broad intense O−H stretch at 3392 cm^{-1} and a sharp C−OH stretch at 1023 cm^{-1} in the beginning of self-assembly. By contrast, Figure 5b

(39) Silverstein, R. M.; Bassler, G. C.; Morrill, T. C. *Spectrometric Identification of Organic Compounds*, 5th ed.; John Wiley: New York, 1991; p 289.
(40) Philip, D.; Stoddart, J. F. *Angew. Chem., Int. Ed. Engl.* **1996**, *35*, 1154.
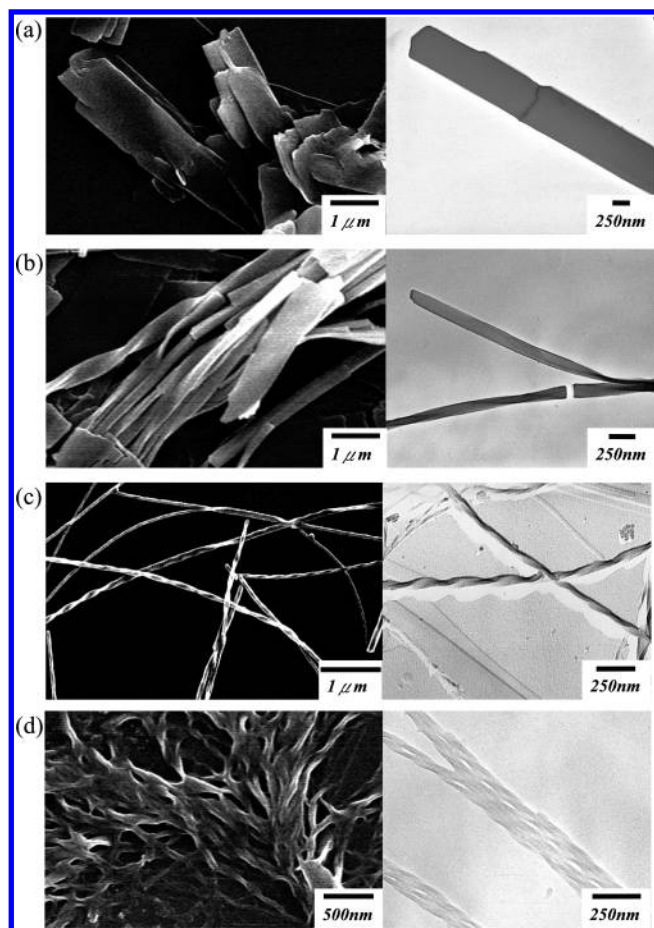
Self-Assembly of Chiral Schiff-based Rod−Coil Amphiphiles

Chem. Mater., Vol. 18, No. 2, 2006 357

Figure 6. FESEM (left) and TEM (right) micrographs of compounds (a) **1a**, (b) **1c**, (c) **1e**, and (d) **1g**.

demonstrates the effect of the hydrogen-bonding interaction, with the 3392 cm^{-1} band (O−H stretch) becoming stronger in intensity and slightly shifting to 3372 cm^{-1}, whereas the 1023 cm^{-1} (C−OH stretching) shifts to 1021 cm^{-1} for the late stage of self-assembly. Obviously, the chiral Schiff-based rod−coil amphiphiles were gradually aggregated in dilute solution as a result of the liquid-crystalline-like behavior combining with the participation of water. Consistent with the spectroscopic observations, the resulting solution gradually turned cloudy within a few hours while the chiral Schiff-based rod−coil amphiphiles was suspended in the THF/H$_2$O mixed solution. The time-resolved UV analyses suggest that the liquid-crystalline-like behavior is driven by the change in the concentration of the molecules in solution upon standing.

Effect of Alkoxyl Chain Length on Self-Assembled Morphology. The self-assembled morphology of the chiral Schiff-based rod−coil amphiphiles in solution was examined by TEM and FESEM. An interesting morphological evolution was identified according to the change of the alkoxyl chain length. At low alkoxyl chain length (i.e., compounds **1a** and **1b**), the self-assembled morphology exhibited a typical liquid-crystalline texture, a platelet-like morphology (illustrated in Figure 6a). However, helical twists were identified once the alkoxyl chain length reached a certain value. The self-assembly of chiral Schiff-based rod−coil amphiphiles having longer alkoxyl chain lengths (i.e., compounds **1c** and **1d**) exhibited a mixed morphology including a platelet-like morphology and left-handed helical twists. The

amphiphiles of **1c** having an alkoxyl chain length of $n = 9$ presented the behavior of a transitional composition for the self-assembled morphology. Figure 6b illustrates the self-assembled morphology of compound **1c**, where the helical morphology mainly adopts left-handed helical twists. By contrast, the micrographs of compound **1e** exhibited a left-handed helical morphology in the majority (Figure 6c). The morphologies of **1e** and **1f** were confirmed as left-handed helical morphological textures. Figure 6d shows further fine and left-handed helical aggregated structure of compound **1g** (i.e., alkoxyl chain length of 13). The hierarchical aggregates composed of several helical strands were further visualized in the FESEM and TEM micrographs. In general, hierarchical self-assembly is common in biological systems. A well-known example is the formation of collagen, in which every three α-helix chains fold into triple-stranded helixes, which then self-assemble into collagen fibers. Similarly, a hierarchical twisting morphology through the transfer of chiral information from the chain conformation to the phase level was identified in our self-assembly system. It is also noted that the pitch length of the helical twists decreases with increasing alkoxyl chain length. Moreover, the formation of a fine helical morphology significantly depends on the chain length being sufficient but is independent of an odd−even chain length effect. This is in line with the UV and CD observations. Therefore, the liquid-crystalline-like behavior attributed to the Schiff-based entity is driven by the change in concentration of the molecules in solution upon standing. Significant helical twisting could be achieved by introducing longer alkoxyl chains. Consequently, the formation of helical twists is induced by the chiral entities of the amphiphiles, namely, the sugar-based entities. We conclude that chirality plays a crucial role in the self-assembly of a helical morphology.

On the basis of morphological observations and spectroscopic results, speculation was made that the self-assembly is driven by hydrogen-bonding intermolecular interactions and amplified by $\pi-\pi$ interactions leading to liquid-crystalline-like aggregation so as to stabilize the morphology, whereas the sugar moieties create the chiral activity to form the helical morphology. We thus assume that the aggregation mechanism is driven by lyotropic-like behavior.

Molecular Dispositions of Self-Assembled Superstructures. To visualize the molecular dispositions of the self-assembled superstructures from the chiral Schiff-based rod−coil amphiphiles, molecular simulations were performed using HyperChem 7 with the OPLS force field. Compound **1e** was selected as a standard to briefly evaluate the chiral effect during self-assembly. Figure 7 illustrates the molecular modeling results of self-assembled systems. As shown, the helical twists are formed by the self-assembly of the smectic-like bilayer characteristic having parallel alkoxyl groups and parallel phenyl moieties as well as loosely packed sugar entities, which is consistent with the spectroscopic analyses. Evidence for the smectic-like bilayer characteristic can also be identified by small-angle X-ray scattering (SAXS), and detailed studies with respect to the smectic-like morphologies, particularly in the bulk state, are still in progress. According to the simulated layered structure, the thickness of the smectic-like bilayer was estimated as 5.68 nm. Compared to the experimental results according to which
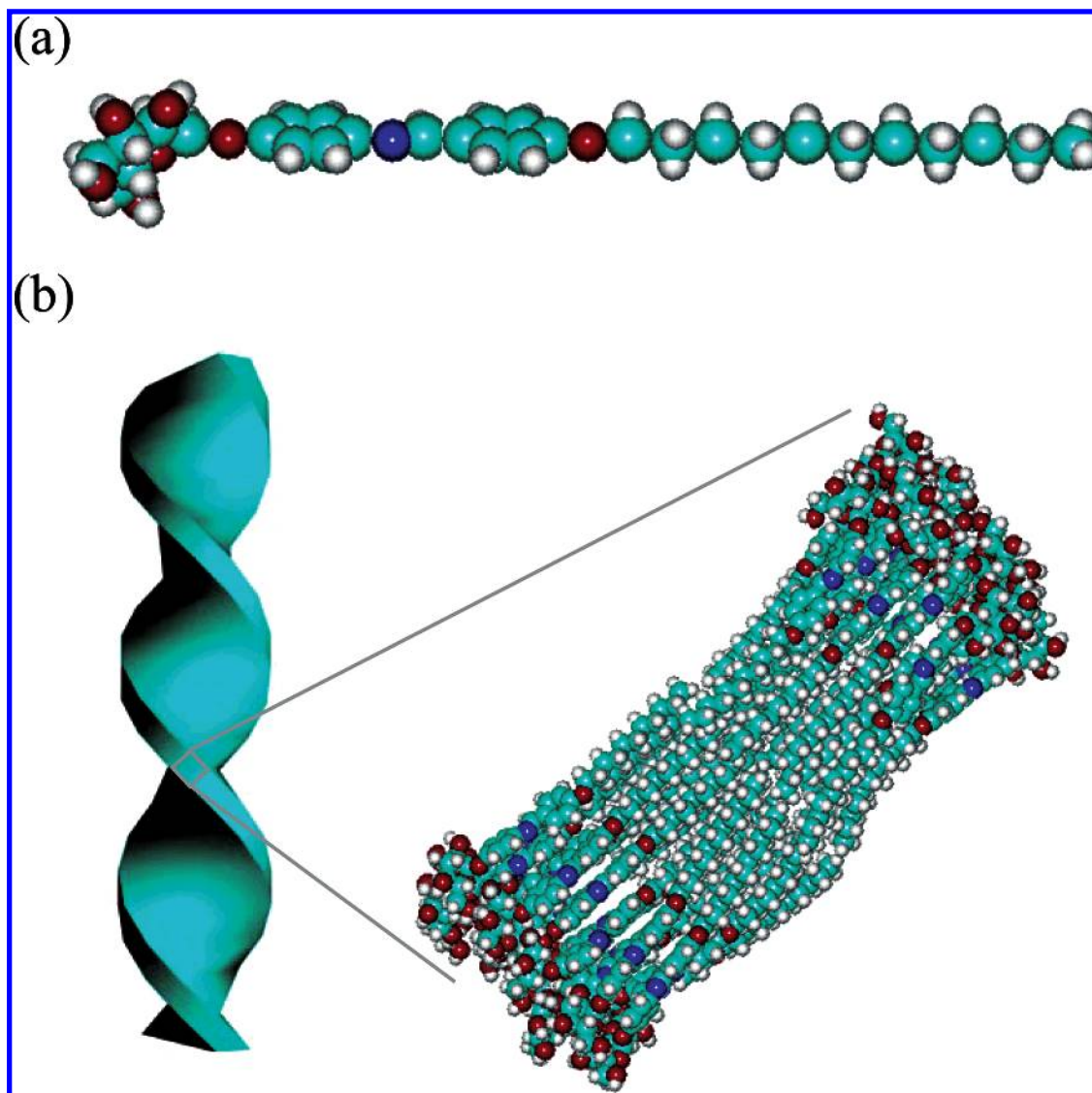
Figure 7. Molecular simulation results for (a) single chiral Schiff-based rod−coil amphiphiles, (b) aggregate morphology in the self-assembly system.

the thickness of the layered superstructure was in the range of 30−50 nm, the resulting morphology might be built up of six to nine layers of the smectic-like bilayer. The bending curvature of the self-assembled chiral bilayer is induced by the chiral sugars and amplified by the Schiff-based rod−coil segregation, so that significant bending could be achieved by introducing long enough alkoxyl chains. Consistent with the theoretical prediction,[41−45] the bending force from the chiral entities depends on the sizes of the adjacent hydrophobic tails and hydrophilic headgroups in the chiral lipid bilayer molecules. The molecular dispositions of twisting and bending chiral Schiff-based rod−coil amphiphiles are indicated in Figure 8. Theoretical discussions have suggested that the twisting of the smectic-like bilayer is carried out on the $1 \rightarrow 2$ plane. By contrast, the formation of the bending curvature of the smectic-like bilayer is in the $2 \rightarrow 2'$ plane. Such twisting is equivalent to stereo hindrance in a short-range correction. Similarly, the bending curvature

requires two-dimensional bilayer membranes with a long-range correction, resulting in the formation of a helical morphology. Recently, a systematic study of chiral self-assembly through Monte Carlo simulations on the basis of a mesoscopic approach was carried out by Selinger and co-workers.[46] The self-assembled morphology with a helical sense from the growth of an aggregate from solution can be clearly determined by a complex interplay between elastic forces and the orientation and chirality of the constituent molecules. Different helical aggregates with various pitch lengths and diameters can be found by varying the tilt direction with respect to the crystallographic axes. Considering the occurrence of self-assembly tilting, we thus suggest that our chiral Schiff-based rod−coil amphiphiles could self-assemble to form a smectic-like bilayer for helical structures and the pitch length of the helical twists thus decreases with increasing alkoxyl chain because of the intensification of bending force. That is, the size of the alkoxyl chain determines the threshold of bending for the formation of a helical morphology.

(41) Yang, Z. C. O.; Liu, J. X. *Phys. Rev. Lett.* **1990**, *65*, 1679.
(42) Selinger, J. V.; Schnur. J. M. *Phys. Rev. Lett.* **1993**, *71*, 4091.
(43) Nandi, N.; Bagchi, B. *J. Am. Chem. Soc.* **1996**, *118*, 11208.
(44) Selinger, J. V.; MacKintosh, F. C.; Schnur, J. M. *Phys. Rev. E* **1996**, *53*, 3804.
(45) Nandi, N.; Bagchi, B. *J. Phys. Chem. A* **1997**, *101*, 1343.

(46) Selinger, R. L. B.; Selinger, J. V.; Malanoski, A. P.; Schnur. J. M. *Phys. Rev. Lett.* **2004**, *93*, 158103-1.
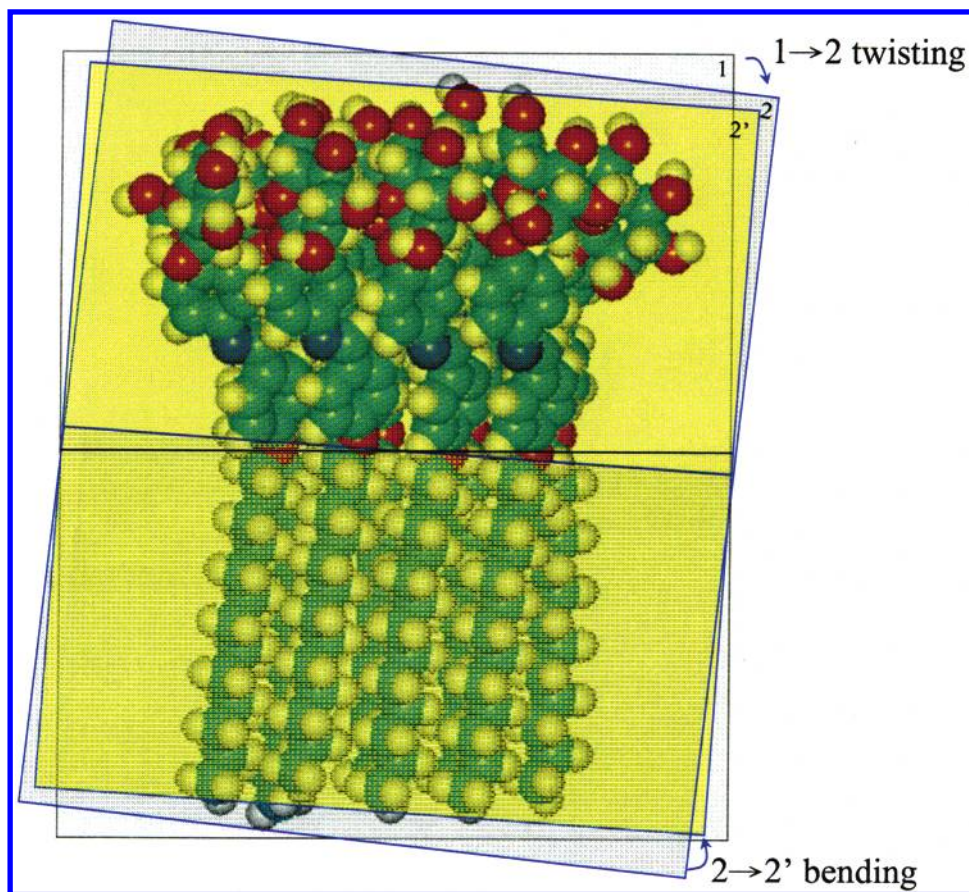
Figure 8. Twisting and bending chiral Schiff-based rod−coil amphiphiles of compound **1g**.
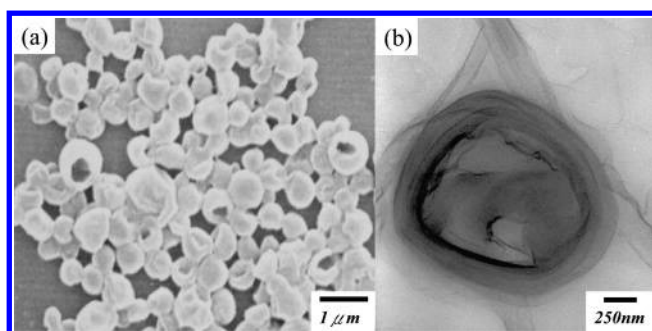

Figure 9. (a) FESEM and (b) TEM micrographs of spherical vesicles.

Vesicular Morphology from Swallow-Tail Molecules. In addition to examining the effect of chain length in the self-assembly results, we attempted to alter the chain number by introducing additional alkoxyl chains with equal lengths in a nearby phenyl position to investigate the influence of self-assembling blocks caused by an asymmetry in molecular geometry. Herein, a 3,4-diundecyloxybenzlidene aminophenyl-α-d-glucopyranoside (compound **2**, $n = 11$) was synthesized to compare with the linear sharp compound **1e** for the ability to form a classical helical morphology. Following a similar self-assembly process, a dramatic change of the bilayer aggregates appeared in compound **2**. Spherical vesicles with a relatively uniform distribution of sizes about 0.5-μm diameter were observed by FESEM (Figure 9a). Apparently, the additional side chain has a discernible effect on the aggregated morphology. To further confirm the vesicular morphology, a TEM image (Figure 9b) reveals an obvious contrast between the periphery and the center of the sphere, suggesting the projection image of a hollow sphere. The thickness of the sphere is evaluated to be about 200−250 nm. We speculate that the observed discrepancy is very likely to be due to the additional long flexible alkoxy tether asymmetrically involved, thus inducing the collapse of the twisted shape into spherical micelles.

Conclusion

We have synthesized a series of chiral Schiff-based rod−coil amphiphiles with different alkoxyl chain lengths that exhibit liquid-crystalline-like behavior for self-assembly so as to create tunable self-assembled morphologies including platelet-like morphologies, helical twists, and vesicular textures. The results described here demonstrate that amphiphilic Schiff-based molecules with a small hydrophilic part assemble into well-defined morphologies by tuning the alkoxyl chain length. Increasing the chain number of alkoxyl chains induces the collapse of the helical twists into vesicular micelles. Biomimicking from nature, the introduction of chiral entities provides one convenient way of creating a variety of morphologies, particularly helical twists.